

SPECTRALLY RESOLVED SOLAR IRRADIANCE DERIVED FROM METEOSAT CLOUD INFORMATION - METHODS AND VALIDATION

Jethro Betcke*, Tanja Behrendt, Jan Kühnert, Annette Hammer, Elke Lorenz, Detlev Heinemann

Carl von Ossietzky University Oldenburg, Energy and Semiconductor Laboratory,
Energy Meteorology Group, *Corresponding Author: Jethro.Betcke@uni-oldenburg.de

Abstract

The varying spectral distribution of the terrestrial irradiance can cause significant differences between the actual and the rated efficiency of solar cells. To account for this effect it is necessary to calculate the weighted irradiance which depends on the solar cell spectral response and on the spectral distribution of the irradiance. Because ground based spectral measurements are sparse, satellite based spectral data can provide a good alternative. In this work we have compared two approaches.

The SOLIS method can calculate both broadband and spectrally resolved terrestrial solar irradiance from satellite data. The clear sky module of SOLIS is based on a partial parametrisation of radiative transfer calculations, and uses atmospheric data from climatologies or satellite based methods. The cloud module is based on empirical relationships between the cloud albedo values determined from Meteosat visual channels and the cloud transmittance. In parallel we developed a simpler empirical method, that can be more easily implemented in photovoltaic modelling software. It is based on principal component analysis of measured spectrally resolved irradiance and empirical relationships between the principal components and satellite derived clear sky index and sun elevation.

Both methods have been validated using the same ground measured data from Stuttgart Germany. The weighted irradiance has been used as metrics to compare the results of the models. It was found that the use of both models gave a significant improvement compared to the use of a constant AM1.5 spectrum. The use of the empirical model resulted in lower bias values, the use of SOLIS resulted in lower RMSE values.

INTRODUCTION

Spectrally resolved solar irradiance data are an essential input for a variety of applications such as the modelling of plant growth, climate modelling and the simulation of photovoltaic solar energy systems. In this paper we will focus on the latter, but the models themselves are not limited to this application.

The rated efficiency of a photovoltaic module is measured using the standard AM 1.5 spectrum [1]. In contrast, the spectrum experienced under working conditions will have strong temporal and spatial variations. Especially for solar cells with a narrow spectral response such as amorphous silicon (see Fig. 1), this implies that the efficiency in the field can differ considerably from laboratory results and annual yields can vary up to 10% from expected values [6][15]. Measurements of the spectral distribution of solar irradiance are however too scarce to be used for the simulation of an arbitrary PV system. Spectral models based on satellite data therefore provide a potential alternative.

At Oldenburg University two such models have been developed. The SOLIS model [2][14] is based on radiative transfer modelling and has the potential for a higher accuracy. A new empirical model is expected to be less accurate than SOLIS, but its simplicity allows integration in PV simulation software.

The goal of this work is to validate the two spectral methods, and compare the results. In the following sections we will present the used data, introduce the metrics for the validation, introduce the two spectral models, present and discuss the validation results, and finally present the conclusions.

Dataset	Loughborough	Stuttgart
Location	52.77°N, -1.23°E	48.75°N, 9.11°E
Provided by	CREST, Loughborough University [5]	IPE, Stuttgart University
Period	sept 2003- Aug 2004	2008
Apparatus	Horiba, custom build	Stellarnet EPP 2000C UV-VIS, EPP 2000 NIR INGAS
Temporal resolution	2 min. scan, every 10min.	1 min. scan every min., delivered as 15 min. average
Spectral resolution	10 nm	1 nm
Spectral range	300 to 1700 nm	300 to 1700 nm
Orientation	20° East	South
Tilt	52°	33°
Completeness original data	35 %	98 %
Completeness hourly data	40 %	97 %

Table 1: Description of the datasets used for this investigation. Note that the difference in completeness between the original and the hourly data is caused by the fact that only hours with at least two data points have been used for the hourly average.

DATA

For this work we used two data sets consisting of one year of spectral measurements. Both are described in Table 1. To make them comparable they were averaged to hourly values. The Loughborough data set was only used as learning dataset for the empirical spectral model. The Stuttgart dataset was used for the validation of both models. Both data sets were quality checked by the institutes that carried out the measurements.

SPECTRAL EFFECT ON SOLAR CELLS

The efficiency of solar cells is rated under standard test conditions using the so-called AM1.5 spectrum. However, under field conditions the efficiency of solar cells depends on the spectral distribution of the irradiance and the spectral response of the applied material. The spectral response $SR(\lambda)$ of solar cells is defined by the response of the short cut current to different wavelengths. Examples for four types of solar cells are shown in Fig. 1.

When the normalised spectral irradiance $n(\lambda)$ and $SR(\lambda)$ are known the short circuit current (I_{sc}) can be calculated from the rated short circuit current ($I_{SC,AM1.5}$) using:

$$I_{SC} = iSMMF \cdot I_{SC,AM1.5} = I_{SC,AM1.5} \cdot \frac{\int SR(\lambda) n(\lambda) d\lambda}{\int SR(\lambda) n_{AM1.5}(\lambda) d\lambda} \quad (1)$$

where $iSMMF$ is the inverse spectral mismatch factor. In a first approximation the maximum power output P_{mpp} of a solar cell is proportional to I_{sc} . We therefore define the weighted irradiance G_w as a measure for the spectral effect on the power output of a PV system:

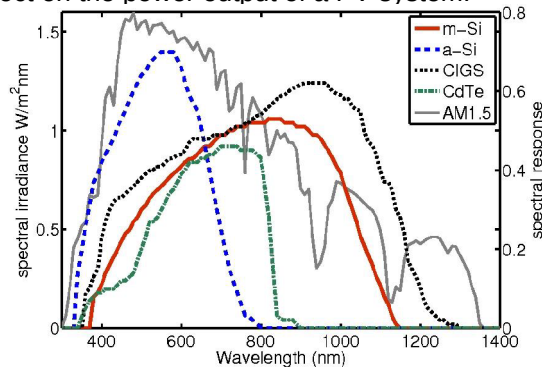


Figure 1: AM1.5 spectrum and the spectral response of four types of solar cells

$$G_w \equiv iSMMF \cdot G \quad (2)$$

Furthermore, it can be shown, that the effect of non-STC spectra can be accounted for by replacing G with G_w as an input for photovoltaic system models [3]. We shall therefore use G_w to assess the accuracy of the spectral models.

HELIOSAT

Both spectral models presented in this paper depend on the Heliosat method [5] to provide information on cloud transmittance. The method uses albedo data measured by geostationary satellites as input. The method consists on three major steps. In the first step a statistical analysis is carried out on a time series of reflectance values to identify clear sky time slots and determine the ground albedo. This process is carried out for each individual pixel. The second step calculates the so-called cloud index n from the apparent albedo ρ , the ground albedo ρ_G and the maximum cloud albedo ρ_C .

$$n = \frac{\rho - \rho_G}{\rho_C - \rho_G} \quad (3)$$

Subsequently an empirical piecewise linear relationship is used to calculate the clear sky index k_t^* from n . The clear sky index is a parameter for the transmittance of clouds and is defined by defined by:

$$k_t^* \equiv \frac{G}{G_{clear}} \quad (4)$$

where: G is the global irradiance and G_{clear} is the global irradiance in the absence of clouds. To account for the difference between total overcast situations and broken cloud situations we applied the spatial variability correction developed by Lorenz [12]. By combining k_t^* derived from the Heliosat method with the clear sky irradiance derived from a clear sky model the global irradiance can be calculated.

For the Loughborough calculations the data of the visual channel of the MVIRI instrument aboard Meteosat 7 was used, for the Stuttgart calculations the high resolution visual channel of the SEVERI instrument aboard Meteosat 8 and Meteosat 9 were used. The adaptation of the Heliosat method to the MSG-SEVIRI instrument is described by Kuhlemann and Hammer [11].

SOLIS

The SOLIS method is able to calculate both broadband and spectrally resolved irradiance from satellite data by combining the spectrally resolved clear sky irradiance from the SOLIS-Clearsky module with the clear sky index of the Heliosat method. An overview on the different modelling steps is given in Fig. 2.

SOLIS-Clearsky [14] module uses the correlated k method [8] as implemented in libRadtran [13] to calculate the spectrally resolved irradiance for solar zenith angles (θ_z) of 0° and 60° . The spectrum is divided into 32 bands of different widths, so called "Kato bands" between 250 nm and 4600 nm in which the absorption coefficient of different gases is almost constant. Climatological data on aerosol, ozone, and water vapour content of the atmosphere serve as input (see Table 2). By fitting the modified Lambert Beer equations to the libRadtran output, and using the found fitparameters to extend the results to other values of θ_z :

$$E_{clear}(\lambda) = E_0(\lambda) \cdot e^{\frac{-\tau_0}{\cos^a(\theta_z)}} \cdot \cos(\theta_z) \quad (5)$$

where: $E_{clear}(\lambda)$ is the spectrally resolved clear sky irradiance, $E_0(\lambda)$ is the extraterrestrial spectral irradiance, τ_0 is the optical depth and a is the modified Lambert Beer parameter. A similar equation is used for the direct irradiance.

To obtain the spectrally resolved irradiance under cloudy conditions the clear sky spectral irradiance is

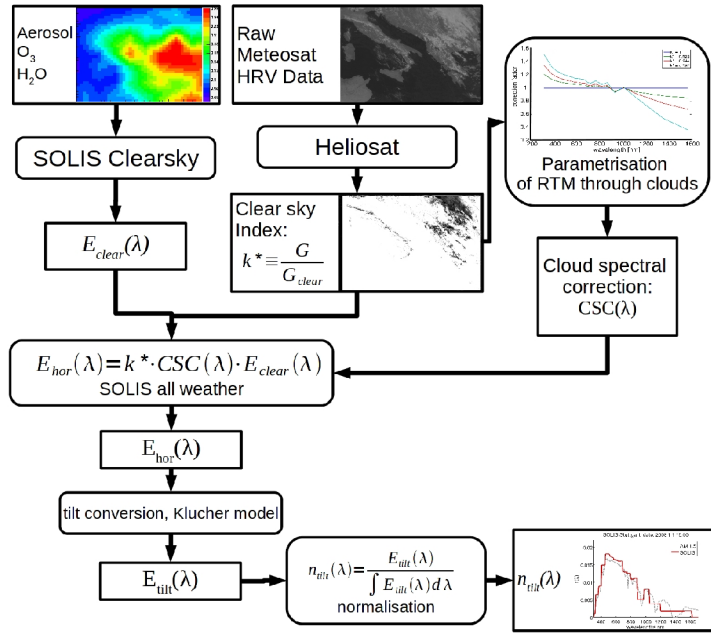


Figure 2: Flow diagram of the SOLIS model.

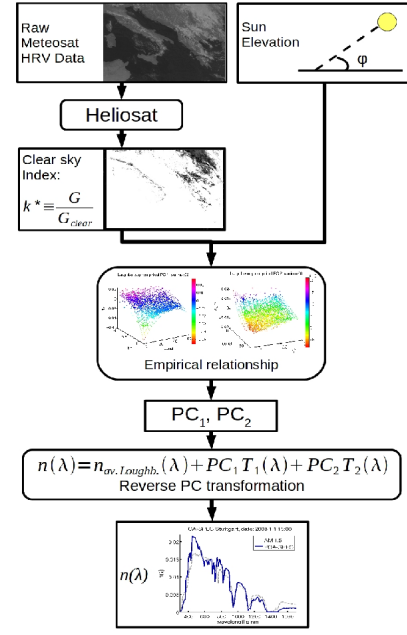


Figure 3: Flow diagram of the empirical spectral model.

multiplied with the clear sky index and a cloud spectral correction $CSC(\lambda, k_t^*)$. The latter is based on a parametrisation of radiative transfer calculations.

$$E_{hor}(\lambda) = k_t^* \cdot CSC(\lambda, k_t^*) \cdot E_{clear}(\lambda) \quad (6)$$

Tilt Conversion

PV-modules are mostly placed on a tilted plane facing the equator. The horizontal spectral irradiance therefore has to be converted to this tilted plane. It consists of the direct, ground reflected and diffuse component. The direct component can be calculated from geometric considerations. An isotropic reflection is assumed for the ground reflected component. The diffuse component is calculated using the Klucher model [10]. All calculations are carried out for each Kato band separately.

EMPIRICAL SPECTRAL MODEL BASED ON PRINCIPAL COMPONENT ANALYSIS

The basic set-up of the empirical model is to describe the spectral distribution with a small set of parameters and determine an empirical relationship between these parameters and the clear sky index and the solar elevation. If the parameters are chosen in such a way that they can be transformed back to a spectral distribution with an acceptable accuracy loss, the spectral distribution can be calculated from the clear sky index and the solar elevation.

Principal Component Analysis of the spectral distribution

Considering the normalised spectral irradiance as a set of 141 correlated variables, we are looking to a linear transformation that maps these onto a new set of parameters that are uncorrelated. These so-called principal components can be found by first determining the eigenvectors of the covariance of the normalised spectrum [7]:

Atmospheric constituent	properties	database	Spatial resolution	Temporal resolution
Aerosols	AOD, single scattering albedo	AEROCOM [9]	1° x 1°	Monthly
Water vapour	column	NVAP [16]	2.5°x2.5°	Monthly
Ozone	column	LibRadtran default		

Table 2: Input used for the SOLIS Clear sky calculations.

$$C_{ij}(e_j)_L = \Lambda_L (e_i)_L \quad \text{with} \quad C_{ij} = \text{cov}(n_{it}, n_{jt}) = \frac{\sum_t^{N_t} (n_{it} - \bar{n}_i)(n_{jt} - \bar{n}_j)}{N_t - 1} \quad (7)$$

where: C_{ij} is the covariance matrix Λ_L is the Lth eigenvalue, $(e_i)_L$ is the Lth eigenvector, $n_{it} = n(\lambda_i, t)$ is the normalised spectrum, \bar{n}_i is the temporal average of the normalised spectrum, and N_t is the number of points in the time series.

The principal components are then defined by the inner-product of the eigenvectors and the normalised spectral irradiance:

$$PC_i(t) = \sum_{j=1}^{140} T_{ij} (n_{jt} - \bar{n}_j) = \sum_{j=1}^{140} (e_j)_i (n_{jt} - \bar{n}_j) \quad (8)$$

The eigenvalues Λ_L equal the variance described by the corresponding principal component. By sorting the eigenvalue-PC pairs by the magnitude of the eigenvalue in decreasing order, the lowest numbered principal component has the largest information content. Application to the Loughborough dataset shows that the first two PCs together describe more than 80% of the total variance. We use these two PCs to efficiently describe the spectrum. An approximated value for the spectrum can be obtained by applying the reverse of the transformation of Eq. 8:

$$n_i^{\text{approx}}(t) = \bar{n}_i + \sum_{j=1}^M T_{ji} PC_j = \bar{n}_i + \sum_{j=1}^M (e_i)_j PC_j \quad (9)$$

where n_i^{approx} is the approximated normalised irradiance, and M is the number of PCs to be considered. For our model we choose $M=2$.

When Eq. 8, with T_{ij} and \bar{n}_i derived from the Loughborough dataset, is applied to the spectral irradiance from Stuttgart, the first two PCs still describe 78% of the variance [3]. This means that the transformation can be carried over to other locations with an acceptable additional information loss.

Empirical relationship

Having established that two principal components can describe the spectrum with an acceptable accuracy, we investigated the relationship between the two principal components of the Loughborough dataset and k_t^* and the sun elevation φ . The relationship can be described in a good approximation with the polynomial :

$$PC_i = \sum_{n=0}^N \sum_{m=0}^M a_{inm} k_t^{*n} \varphi^m \quad (10)$$

where: $N=3$ and $M=2$ for cases when the sun is in front of the module and $M=1$ in case sun is behind the module. The fit coefficients a_{inm} are given in Betcke et al. [3].

With a known average normalised spectrum and known covariance eigenvectors of the spectrum can be determined from these empirical PCs. To investigate if these relationships are also valid at other locations we used equations 10 and 9 with values for T_{ij} , \bar{n}_i and a_{inm} derived at Loughborough, to values of k_t^* and φ determined for Stuttgart. The results are discussed in the next section.

RESULTS AND DISCUSSION

Normalised spectrum

We used SOLIS and the empirical model to calculate an hourly time series of normalised irradiance at the tilted plane in Stuttgart for the year 2008. The results of the models were analysed using the MBE and RMSE per 10nm wavelength band:

$$MBE(\lambda) = \frac{\sum_{t=1}^{N_t} n_t^{\text{model}}(\lambda) - n_t^{\text{meas}}(\lambda)}{N_t} \quad RMSE(\lambda) = \sqrt{\frac{\sum_{t=1}^{N_t} (n_t^{\text{model}}(\lambda) - n_t^{\text{meas}}(\lambda))^2}{N_t}} \quad (11)$$

For the models to have any value they should perform better than a constant AM1.5 spectrum. This is therefore used as a reference model.

The $MBE(\lambda)$ for the three models are shown in Fig. 4. The SOLIS model shows very high values at isolated peaks and at wavelengths from 700nm. This is mainly due to the lower spectral resolution of the model results. Especially at higher wavelengths the Kato bands become too wide to describe the 10 nm resolution data. The isolated extreme MBE values correspond with the edges of the Kato bands.

The empirical model outperforms the AM1.5 spectrum for the larger part of the wavelength range. A first exception is the range below 380 nm. This is likely due to calibration difficulties at the learning data set [2]. Furthermore, there are isolated extremes, that occur where the spectrum shows strong gradients. The most notable occurs at 780 nm, which corresponds with the oxygen absorption band. These are caused by the difference in spectral resolution of the original data between the Loughborough and Stuttgart data set. The Loughborough data were measured at 10 nm intervals, whereas the Stuttgart data were measured at 1 nm intervals and later averaged to 10nm datasets.

The $RMSE(\lambda)$ for the three models are shown in Fig. 5. In the range below 600 nm the SOLIS model outperforms both the AM1.5 as the empirical model. This means that it is better in describing the temporal dynamics in this range. Further improvements are expected if up-to-date atmospheric data are used, rather than climatologies. The range above 800 nm is again dominated by the errors caused by the wide Kato bands. This suggests that the results of the model can be improved by choosing narrower bands in the higher wavelength ranges.

The empirical model gives improvements compared to the AM1.5 spectrum in the ranges between 380 and 600 nm and above 1100 nm. The artefacts originating from the learning data set described for the MBE are also visible in the RMSE. Most likely results can be improved by choosing another learning data set. In the range below 600 nm the RMSE of the empirical model is higher than that of SOLIS. This reflects that the exclusion of the influence atmospheric composition, limit its capability to reproduce the temporal variations of the spectrum. Overall it can be concluded that, with the current set-up of the models, the empirical model gives the best results for a high resolution description of the normalised spectrum.

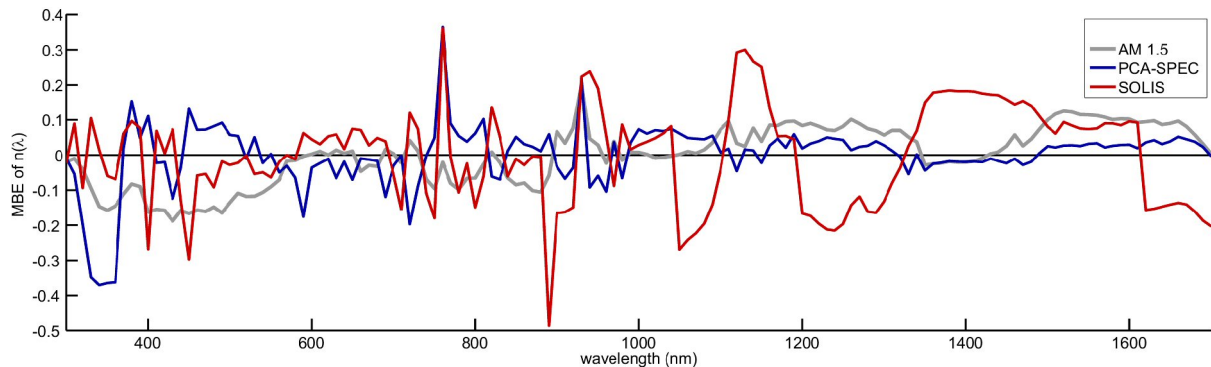
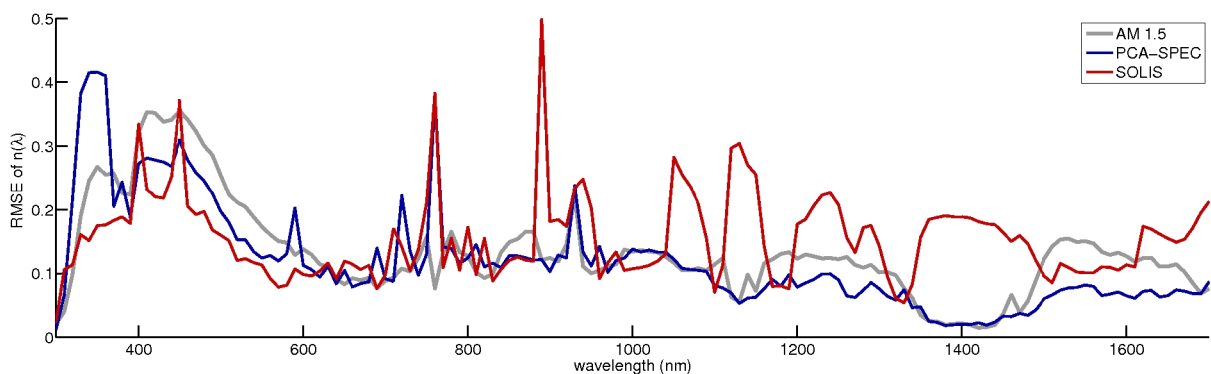


Figure 4: MBE of the normalised spectral irradiance.



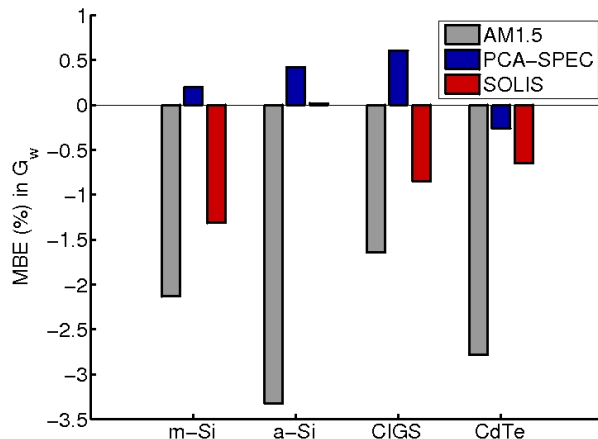


Figure 6 : MBE of the weighted irradiance for four types of solar cells.

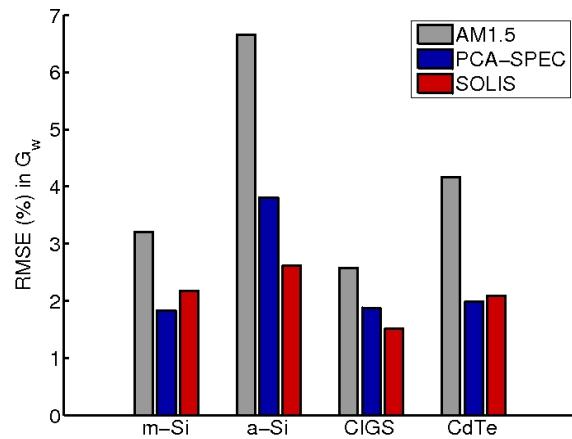


Figure 7: RMSE of the weighted irradiance for four types of solar cells.

Weighted irradiance

To investigate the suitability of the two models for the intended application we used their output to calculate the weighted irradiance defined in Eq. 2 for the types of solar cells displayed in Fig. 1. The values for G were taken from the measurements. We compared the results with G_w calculated directly from the measurements in Stuttgart, and calculated the relative MBE and RMSE.

The MBE results in Fig. 6 show that ignoring the spectral effect, i.e assuming a constant AM1.5 spectral distribution, causes an underestimation of the annual G_w ranging from 1.7% for CIGS to 3.3% for a-Si solar cells. In contrast to the results for the normalised spectrum, both models give considerable improvements upon this use of the AM1.5 spectrum. The difference in results is caused by the weighing with G , because both models are better in describing the spectral distribution for higher values of G . Furthermore it can be seen that, except for the amorphous silicon solar cell (a-Si), the empirical model gives a better result than the SOLIS model.

The RMSE results in Fig. 7 also show significant improvements for both models compared to the constant AM1.5 spectrum. The SOLIS model gives a significantly better result for a-Si, compared to the empirical model. This is caused by the coincidence of the spectral response range of a-Si with the range where the Kato bands are narrow and the SOLIS results are the best. For the other solar cell types the differences are small.

CONCLUSIONS

Ignoring spectral effects in the simulation of photovoltaic solar energy systems can lead to substantial errors in the calculated yield of photovoltaic systems. In our calculations we found underestimations up to 3% of the weighted irradiance, which is a first estimate of the spectral effect on the system output.

Spectral models based on cloud data derived from Meteosat are able to provide the spectral data. We presented the SOLIS model, which is based on radiative transfer calculations, and a new empirical model based on principal component analysis of the normalised spectrum. Both models were validated on one year of hourly spectral data on a tilted plane in Stuttgart Germany. The empirical model gave the most accurate results for the description of the normalised spectrum. Both models give substantial accuracy improvements for the accuracy of the weighted irradiance, and hence the power output, of four types of solar cells. The empirical model is more effective in reducing the MBE, the SOLIS model is more effective in reducing the RMSE.

Improvements for the SOLIS method are expected by using instantaneous and high resolution values for the atmospheric parameters, and by using narrower spectral bands. Improvements for the

empirical model are expected by improvements in the learning dataset, inclusion of the effect of tilt and orientation, and by extending the model with the influences of the atmospheric composition.

ACKNOWLEDGEMENTS

This work has been supported by the Deutsche Bundesstiftung Umwelt. Thomas Betts from CREST, Loughborough, and Bastian Zinßer from IPE Stuttgart, are thanked for providing the spectral measurement data, and Fernando Fabero of CIEMAT Madrid for the solar cell spectral response data.

REFERENCES

- [1] ASTM (2003), G173-03 tables: Extraterrestrial spectrum, terrestrial global 37 deg south facing tilt and direct normal plus circumsolar. Technical report.
- [2] Behrendt, T., Kühnert, J., Hammer, A., Lorenz, E., Betcke, J., and Heinemann, D, (2010) Spectrally resolved solar irradiance from satellite data to investigate the performance of thin film photovoltaics. In Proceedings of the 25th European PV Solar Energy Conference, Valencia. WIP Munich.
- [3] Betcke, J, Hammer, A, Lorenz, E., (2010) An empirical model for the spectral distribution of solar irradiance on a tilted plane based on principal component analysis. to be submitted.
- [4] Betts, T., (2004) Investigation of Photovoltaic Device Operation under Varying Spectral Conditions. Phd thesis Loughborough University.
- [5] Hammer, A., Heinemann, D., Hoyer, C., Kuhleman, R., Lorenz, E., Mueller, R., Beyer, H.g., (2003) Solar Energy Assessment Using Remote Sensing Technologies. *Remote Sensing of Environment*, **86** (3), pp. 423-432.
- [6] Houshyani Hassanzadeh, B., de Keizer, A., Reich, N., van Sark, W., (2007) The Effect of a varying solar spectrum on the energy performance of solar cells. In Proceedings of the 22nd European Photovoltaic Solar Energy Conference.
- [7] Jolliffe, I., (2004) *Principal Component Analysis*. Springer Verlag, 2004.
- [8] Kato, S., Ackerman, T., Mather, J., Clothiaux, E., (1999). The k-distribution method and correlated-k approximation for a short-wave radiative transfer. *Journal of Quantitative Spectroscopy and Radiative Transfer*, **62**(1), pp109–121,
- [9] Kinne, S., Schulz, M., Textor, C., Guibert, S., Balkanski, Y., Bauer, S.E., Berntsen, T., Berglen, T.F., Boucher, O., Chin, M., Collins, W., Dentener, F., Diehl, T., Easter, R., Feichter, J., Fillmore, D., Ghan, S., Ginoux, P., Gong, S., Grini, A., Hendricks, J., Herzog, M., Horowitz, L., Isaksen, I., Iversen, T., Kirkevåg, A., Kloster, S., Koch, D., Kristjansson, J.E., Krol, M., Lauer, A., Lamarque, J.F., Lesins, G., Liu, X., Lohmann, U., Montanaro, V., Myhre, G., Penner, J., Pitari, G., Reddy, S., Seland, Ø., Stier, P., Takemura, T., and Tie, X., (2006) An AeroCom initial assessment optical properties in aerosol component modules of global models., *Atmospheric Chemistry and Physics*, **6**, pp. 1815-1834.
- [10] Klucher, T., (1979) Evaluation of models to predict insolation on tilted surfaces. *Solar Energy*, **23**, pp. 111-1144.
- [11] Kuhlemann R. and Hammer, A., (2005) *Sunsat*, the new program for processing high resolution data of Meteosat-8, technical report to the Heliosat3 project. Carl von Ossietzky University of Oldenburg, Energy and semiconductor Laboratory, Oldenburg, Germany.
- [12] Lorenz, E., (2004) Improved diffuse radiation model. report to the pvsat2 project. Carl von Ossietzky University of Oldenburg, Energy and Semiconductor Laboratory, Oldenburg, Germany.
- [13] Mayer B., Kylling, A., (2005), The libRadtran software package for radiative transfer calculations: Description and examples of use. *Atmospheric Chemistry and Physics*, **5**, pp. 1855–1877.
- [14] Mueller, R., Dagestad, K.F., Ineichen, P., Schroedter-Homscheidt, M., Cros, S., Dumortier, D., Kuhlemann, R., Olseth, J., Pernavieja, G., Reise, C., Wald, L., Heinemann, D., (2004) Rethinking satellite based solar irradiance modelling - the SOLIS clear-sky module. *Remote Sensing of Environment*, **91**(2), pp. 160-174.
- [15] Perez-Lopez, J., Fabero, F., Chenlo, F., (2007) Experimental Solar Spectral Irradiance until 2500nm: Results and Influence on the PV Conversion of Different Materials. *Progress in Photovoltaics. Research and Application*, **15**, pp. 303-315.
- [16] Randel, D. L., T. H. von der Haar, M. A. Ringerud, G. L. Stephens, T. J. Greenwald, and C. L. Combs, 1996: A new global water vapor dataset. *Bulletin of the American Meteorological Society*, **77**, pp. 1233–1246.